HiSST: 2nd International Conference on
High-Speed Vehicle Science Technology
11–15 September 2022, Bruges, Belgium

Development and Testing of an economical Leading-Edge Material for experimental Hypersonic Flight Missions

T. Ruhe [1], H. Elsäßer [2], R. Jemmali [3], L. Klopsch [4], F. Kessel [5], B. Esser [6], A. Gülhan [7]

Abstract

This document presents an overview of the development and testing of a cost-effective material for hypersonic application leading edges by edge Rocket Technology GmbH. Main challenges for a midterm hypersonic flight trajectory are high aerothermal loads and in parallel to stay true to form while handling the thermal management of the overall system including cold structure. The herein designed carbon/carbon-based material (named: '*edgeM13*') was successfully tested in the arc heated facility (L2K) of the Supersonic and Hypersonic Technologies Department at the German Aerospace Centre (DLR) in Cologne. Furthermore, the DLR Institute of Structures and Design, department: Ceramic Composites Structures in Stuttgart analysis the inner structure of the tested specimen via computer tomography and determines the raw material properties. The samples where tested with an equivalent Mach 8 stagnation point heat flux for t=120s in a comparable flight atmosphere of approx. H=40km. The results of the experiments are introduced in detail in this paper.

Keywords: *Hypersonic Leading-Edge, Sounding Rocket Fin, Carbon Fiber Reinforced Ceramic, High Enthalpy Flows, Arc Heated Facility L2K, Computer Tomography Analysis*

Nomenclature

AIAA – American Institute of Aeronautics and Astronautics
C – Thermal Capacity
C/C – Carbon reinforced Carbon
CFRP – Carbon Fiber Reinforced Plastic
CMC – Ceramic Matrix Composites
CT – Computer Tomography
CTE – Coefficient of Thermal Expansion
D – Distance
d – Diameter
DLR – German Aerospace Centre
E – Young's Modulus
ε – Strain
ECSS – European Coorperation for Space Standartization
FEA – Finite Element Analysis
GFRP – Glass Fiber Reinforced Plastic
H – Altitude, Height
h – Specific Enthalpy
κ – Thermal Conductivity

[1] *edge Rocket Technology GmbH, Lämmleshalde 19, 71083 Herrenberg Germany, tobias.ruhe@edge-rocket-tech.com*
[2] *edge Rocket Technology GmbH, Lämmleshalde 19, 71083 Herrenberg Germany, henning.elsaesser@edge-rocket-tech.com*
[3] *German Aerospace Center (DLR) – Institute of Structures and Design – Department: Ceramic Composites and Structures, Pfaffenwaldring 38-40, 70569 Stuttgart, Germany, raouf.jemmali@dlr.de*
[4] *German Aerospace Center (DLR) – Institute of Structures and Design – Department: Ceramic Composites and Structures, Pfaffenwaldring 28-40, 70569 Stuttgart, Germany, linda.klopsch@dlr.de*
[5] *German Aerospace Center (DLR) – Institute of Structures and Design – Department: Ceramic Composites and Structures, Pfaffenwaldring 28-40, 70569 Stuttgart, Germany, fiona.kessel@dlr.de*
[6] *German Aerospace Center (DLR) – Institute of Aerodynamics and Flow Technology, Department: Supersonic and Hypersonic Technology, Linder Höhe, 51147 Cologne, Germany, burkard.esser@dlr.de*
[7] *German Aerospace Center (DLR) – Institute of Aerodynamics and Flow Technology, Department: Supersonic and Hypersonic Technology, Linder Höhe, 51147 Cologne, Germany, ali.guehlhan@dlr.de*

L – Length
ṁ – Mass Flow Rate
Ma – Mach
m% – Mass Percent
NASA – National Aeronautics and Space Administration
P – Pressure
R&D – Research and Development
ρ – Density
Φ – Porosity
σ – Stess
SF – Safety Factor
SiC – Silicon Carbide
T – Temperature
t – Thickness, Time
TPS – Thermal Protection System
V&V – Validation and Verification
v% – Volume Percent
W – Width

1. Introduction

Sounding Rockets are the most important mean to determine, test and prove hardware under real condition - a cost-effective way to hypersonics. Application fields are for example: material research and development, flight-/aerodynamics (e.g. air flow), navigation and flight control for innovative flightpaths, structures and designs (e.g. active or passive thermal management, heat signatures), validation and verification of numerical simulations and diagnostic models, advanced sensors and communication or enhanced ignition and combustion. Hence, it is indispensable to support the possibility for flight experiments, which want to test their systems in a respective environment. Therefore, most important drivers are reliability and a price tag, which is affordable for the whole research community.

Under development of these hypersonic technologies, sounding rocket trajectories become more and more challenging. While in standard sounding rocket missions (e.g. µg-research), metallic leading edges covered by thermal protection systems are valid, but for trajectories including a stable descent this is not reliable anymore. For those trajectories, specialized glass and carbon fiber reinforced phenolics were developed in the mid 60´s and are in use up to today [9]. With the upcoming hypersonic flight envelopes, even those materials are on the limits. To fly in this speed range constantly ceramic matrix composites (C/C-SiC) are used for exposed structures. Those are not only in aspects of material cost intensive, but also in engineering the overall interface management to the cold structure. Especially, the heat input to the cold structure due to the thermal conductivity of the C/C-SiC is a major problem and leads to a premature failure. Therefore, the focus is on the need of new balanced materials in combination with thermal stable junctions to protect the system behind.

Further disadvantages of C/C-SiC are generally long lead times of processing, manufacturing effort and limited machining possibilities. To close this gap between the glass fiber reinforced plastic phenolics and the cost intensive C/C-SiC material, a new material is developed to enable mid-term hypersonic flights with straightforward interface mechanics and thermal management. In addition, the advantages of a fiber-reinforced ceramic such as thermal shock resistance and quasi-ductile fracture behavior are retained. All this covered by an available industrial manufacturing process, optimized for low processing time and cost-effective production (e.g. interface tolerance, thermal and mechanical engineering, standard machining etc.).

The developed material is described and successfully tested on basis of a sounding rocket fin leading edge including a common blade aluminum substructure and its TPS to represent the whole system.

2. Requirements and Material Design

Besides the low weight and cost-efficient needs, for an aerodynamic stable flight the following technical main drivers are determined [1], [9]:

- Thermomechanical resistance up to T=2400°C
- True to form leading edge as required for the respective flight envelope
- Optimized thermal conductivity to protect the cold structure
- Coefficient of thermal expansion and stiffness compatibility to substructure without buckling and critical thermal induced stresses

Starting with the first requirement – resistance up to T=2400°C – restricts the possibilities to whether a CMC or an ablative material.

As a further sub-requirement, the critical thermal path for the cold-structure shall not be the leading edge but a common phenolic-cork TPS at the blade. Depending on the detailed fin design, this gives a limit in thermal conductivity of approx. 0.5 – 1W/mK. A lower conductivity would not lead to a longer possible flight time (Fig 1).

This thermal conductivity requirement in combination with the need of an easily accessible industrial product disqualifies the common CMC´s (e.g. C/C-SiC, UHTCMC etc.). The ablatives design concentrates on carbon fiber-based materials, as this is an easy and in a wide range accessible industrial product in combination with a phenolic matrix.

Due to the requirement – true to form – and the fact, that the ablation takes place under mechanical load, the fiber structure shall be reinforced by a minimum carbon matrix to give a sufficient mechanical support during the phenolic ablation process and resist any deformation during flight [9].

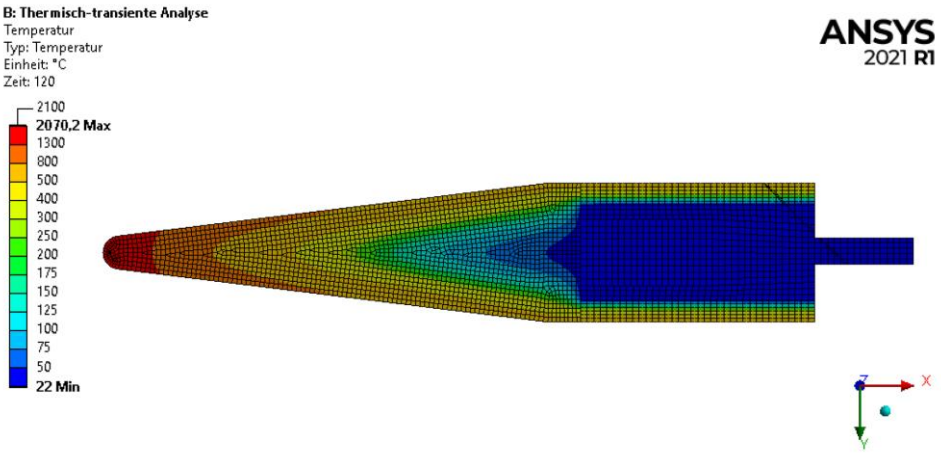

Fig 1. edge Rocket Technology FEA of L2K arc heated test sample (cut view at t=120s)

Regarding thermal induced stresses, a carbon fiber reinforce plastic based substructure would be an optimum as both have a compatible CTE. To be cost effective this leading edge has to work with an aluminium hybrid substructure, as mentioned above.

Following the trajectory – after the launch the leading edge will heat up while the substructure stays cold. During the flight the blade material will slowly heat up, assuming a max. temperature of ΔT=200°C at the aluminum structure, while already cooling down of the leading edge. This introduces a thermal strain at the aluminum of approx. 0,42%. The new material has to allow this thermal strain plus 0.3% of bending strain (0.72% in total) along the leading edge interface with a safety factor of SF=3 [11]. As a further advantage of the low CTE of carbon fiber-based materials: for both thermal flight conditions there is no compressive force on the leading edge that could induce buckling to the leading edge as e.g. seen in the SHEFEX-1 descent with a heated metallic leading edge [1], Fig 2.

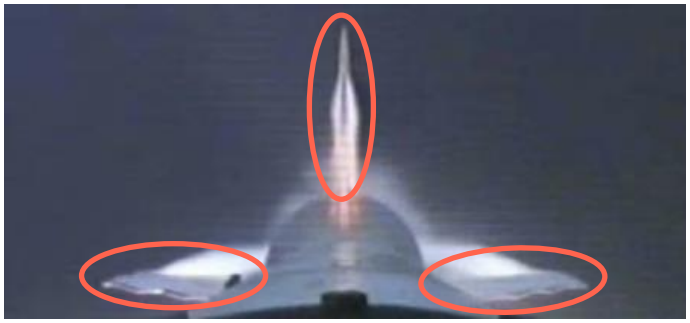

Fig 2. SHEFEX-1 - 2nd-Stage fins during re-entry at approx. Ma=6-7 at H=20km altitude – Buckling of the metallic leading edges [1]

Thermal conductivity and allowable strain can be optimized through fiber volume content, fiber orientation and fiber type itself. Even using all of these possibilities, in the end these two constraints (thermal conductivity and allowable strain) contradict each other and cannot be fulfilled at the same time. Especially, the thermal management due to the higher conductivity was challenging and limited the allowable flight time under hypersonic conditions. The ablative cooling effect of the infiltrated phenolic resin balances the higher thermal conductivity to extend the allowable flight envelope [8]. As a further advantage, the matrix porosity and type can be adapted to a minimum overall density.

3. Experimental Tools and Test Approach

3.1 Test Sample Geometry

The sample geometry is chosen to be symmetrical for reliable FEA recalculation with a perpendicular flow direction. The overall size is optimized to the wind tunnel requirements (see Fig 3). This perpendicular flow (worst case scenario) leads to higher thermal loads in relation to leading edges in common flight hardware, which use to have a sweep angle. Beside the leading edge itself, the cold-structure interface incl. TPS is included and part of the full approach. Fig 4 shows two side views of one entire test sample for experiments in the L2K facility. Two identical samples (A and B) are tested.

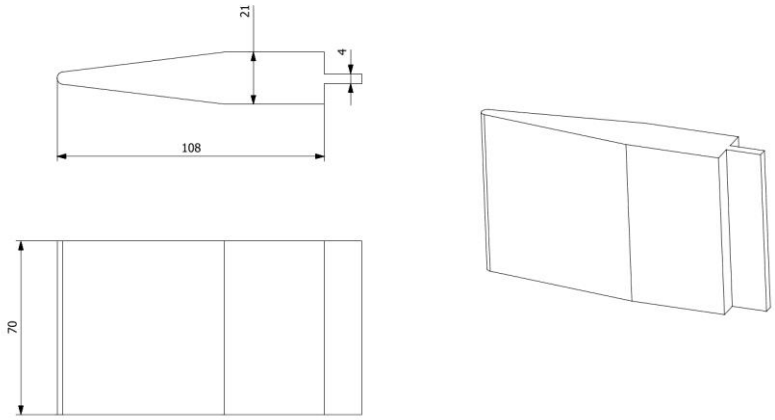

Fig 3. edge Rocket Technology wind tunnel test sample geometry

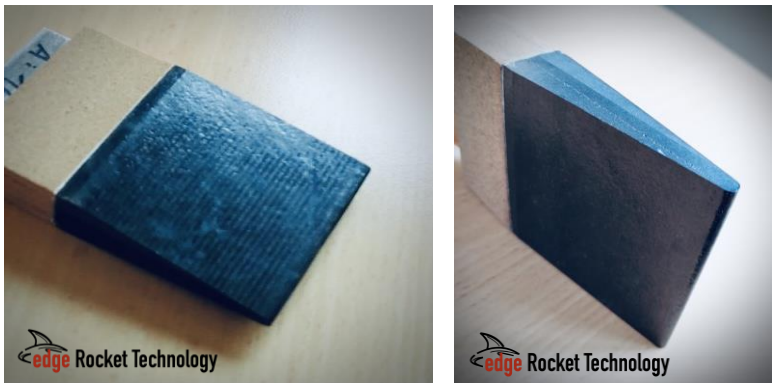

Fig 4. edge Rocket Technology wind tunnel test samples – C/C reinforced leading edge including the developed junction to a respective aluminum blade structure and cork TPS

3.2 Arc Heated Wind Tunnel L2K

In order to perform experiments in a flight relevant test environment, tests were carried out at new test conditions of the arc heated wind tunnel L2K. All test parameters will be described in more details later.

For material tests in a realistic aerothermal environment during re-entry flights the German Aerospace Centre (DLR) uses its L2K and L3K facilities, which are the two test legs of DLR's arc heated facility complex LBK. The setup of LBK is schematically shown in Fig 5 [2, 3, 4]. The L3K facility uses a segmented type arc heater with a maximum electrical power of 6MW that allows achieving cold wall heat flux rates of up to 16MW/m² at stagnation pressures up to 2500hPa. Stagnation point test samples with a diameter up to 100mm and plat plate test with a size of 280mm (W) x 350mm (L) x 70mm (H) can be tested in a homogeneous hypersonic flow field in this facility. Combinations of the same throats and nozzle exit diameters of 50mm, 100mm, 200mm, and 300mm provide Mach numbers between 3 and 10 at Reynolds numbers up to 10000/m.

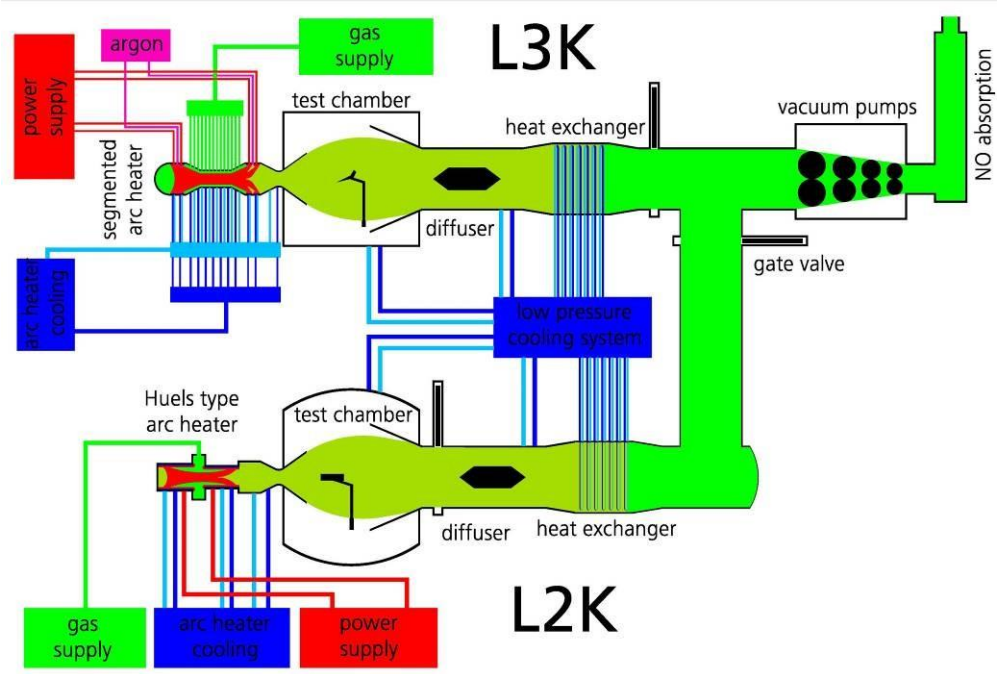

Fig 5. Sketch of the L2K/L3K facilities

The L2K facility on the other site uses a Huels-type arc heater with a maximum electrical power of 1.4MW to energise the working gas to high enthalpy conditions and achieves cold wall heat fluxes up to 3.0 MW/m² at stagnation point pressures of up to 250hPa. Hypersonic free stream velocities are provided by a convergent-divergent nozzle. The nozzle's expansion part is conical with a half angle of 12°. Different throat diameters of 14mm, 20mm, 25mm and 29mm are available and can be combined with nozzle exit diameters of 50mm, 100mm and 200mm. Consequently, the facility setup can be adapted to particular necessities of a certain test campaign. For most aerospace applications of the L2K facility air is used as a working gas. However, there is also continuous and substantial experience in operation with different gases. L2K allows to simulate further atmospheres like Mars, Venus and Titan and to perform tests in pure Argon, Nitrogen and Carbon dioxide environments. The facility includes components for storage and supply of those gases and the corresponding operational parameters are well known.

The application of diagnostic tools for the characterization of high enthalpy flow fields has a long tradition at LBK [5, 6, 7]. Emission spectroscopy, absorption spectroscopy, diode laser absorption spectroscopy, laser induced fluorescence spectroscopy on NO and two photon laser induced fluorescence on oxygen atoms have been applied to air flows providing valuable information on the flow properties. By applying these techniques, rotational and vibrational temperatures, densities, flow

velocities, and shock standoff distances have been measured. The techniques are permanently available and continuously used.
During tests the model is monitored with two optical cameras, one recording the complete flow field and test chamber and the second one recording a close-up of the test sample. For tests with very short testing time or fast ablation mechanisms, a high-speed camera is used. The test sample surface temperature evolution is measured with two different pyrometers. They provide the surface temperature by a non-intrusive measurement based on the assumption of a grey body (two-colour pyrometer) or surface with a given spectral emissivity (spectral pyrometer). Windows integrated into the front flange of the test chamber allow a frontal view onto the sample. Both pyrometers are aligned to the same point at the centre of the sample. The optical measurement can be extended by an infrared-camera, which provides spatially resolved surface temperature information.

3.3 Material Characterization

The mechanical testing of the material was carried out by means of a 3-point bending test in accordance with DIN EN 658-3. 4 specimens with an orientation inside the untested plate material were measured at 0° (comparable to leading edge interface direction). The length to thickness ratio was 20. The test was performed with a universal material testing machine type 1494 from Fa. Zwick/Roell. The test speed was 2mm/min.

For the analysis of the samples tested in the wind tunnel and in order to obtain an estimate regarding the temperatures present in the material in correlation with the degree of pyrolysis that took place in the material, the structure tested under real conditions was axially divided into 16 sections, each of the individual segments having a geometry of 5mm (L) x 4mm (W) x 3mm (H) and thus a volume of 60mm^3. These samples were tested for their mass yield as a function of temperature by means of thermogravimetric analysis in accordance with the DIN EN ISO 11358 standard. An STA 409C from the company Netzsch-Gerätebau GmbH was used for the investigation. [12] The unit operates according to the electromagnetic compensation principle and was operated under an inert atmosphere generated by nitrogen. The measured temperature range is between 20°C and 1450°C, and a heating rate of 10K/min was selected. The cooling is uncontrolled. Starting from the sharp leading edge located directly in the hot gas flow, the numerical value of the samples studied decreases as they move away from the edge. Consequently, the sample numbered 0 was located directly inside the flow (stagnation point), with the sample numbered 16 located outside the test area under the metallic bond.

CT analysis was performed using a v|tome|x L 240/450 CT system (GE Sensing & Inspection Technologies GmbH, Wunstorf, Germany). The microfocus X-ray tube used is capable of a maximum accelerating voltage of 240kV (max. power 320 W). The image receiver is a 16bit area detector with a matrix of amorphous silicon (a-Si) and has 2048x2048 pixels of 0.2mm each.

In addition, the linear thermal expansion coefficient was measured as a function of temperature. This was determined by means of a DIL 402 high-temperature dilatometer from Netzsch-Gerätebau GmbH. The standard used for the determination refers to the expansion properties of ceramic composite materials and is described in DIN EN 1159-1. The measurement method used was the differential method, whereby the change in length of the material sample and a reference sample is determined. [12] The sample geometry was 25mm (L) x 4mm (W) x 3mm (H). The measurement was performed under argon atmosphere and a continuous gas flow of 100ml/min. The start of the measurement was chosen at 25°C, with a heating rate of 5K/min to a maximum temperature of 1500°C. The selected sample material was measured after production, so that no temperature was applied to the sample material yet. In each case, four measurements were made in 0° fiber orientation within the plate material.

4. Results and Discussion

The final '*edgeM13'* material, determined from the requirements (see chapter 2) is produced with the following measured properties before and after the tests.

4.1 Material Properties

The tested specimens show a 3-point bending strength (Table 1) of 65.33MPa in 0° orientation, respectively. A striking feature during material characterization is the high elongation at break, which ranges 2.33% +/-0,13.

Table 1. Mechanical properties of the material depending on the fiber orientation

Material Properties	Orientation 0°
3-Bending Strength [MPa]	65,33 +/- 0,8
Bending Modulus [GPa]	3,76 +/- 0,05
Strain [%]	2,33 +/- 0,13

Analysis of the mass loss that occurred during the hot gas test suggests that the material at the beginning of the sharp edge underwent pyrolysis during the test. The sample with the number 0 retains its mass during the entire course of the test. In comparison, sample number 16 shows a loss of mass in all temperature ranges relevant for pyrolysis to take place (Fig 6). The mass yield approaches a limit value of 60m%. It is striking that the mass yield of the samples increases significantly in the flow direction.

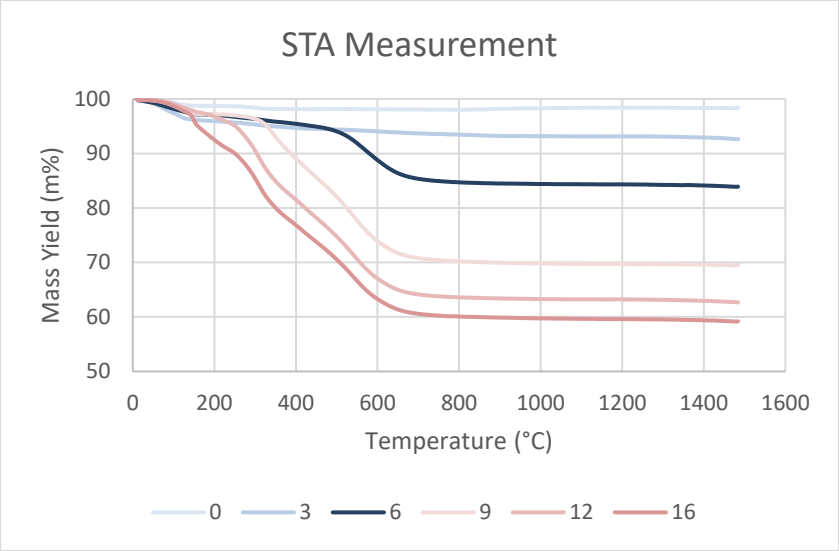

Fig 6. Measurement of the mass yield as a function of the temperature of the sharp leading edge tested in the wind tunnel with numbering the samples ascending in the direction of flow

Based on a model of pyrolysis of phenolic resin reinforced carbon (C/C) structures described by Kimberly, A. et. Al. and Trick, K.A. et. Al., the behavior of mass loss, especially on sample 9 can be illustrated very well. At 300°C, the mass loss of the sample increases sharply until it levels off at a mass yield of 70%. [14, 15] Assuming that under a temperature of 300°C a mass loss of 10m% takes place, it can be seen that this temperature was reached during the test and thus this first mass loss took place. The further mass loss starts in the subsequent STA analysis from 300°C and reaches a limit of 70m% carbon yield. The sharp drop in mass yield for sample 6 in the range of 500°C, suggests that a material temperature of max. 500°C was reached in this range. After 500°C, the main pyrolysis is considered to be complete [13]. In the temperature range >500°C, the benzene rings present within the matrix system are broken up and there is consequently a loss of hydrogen in the material. The high energy input that must occur in this range explains the steep slope in this area of mass loss [14]. Since the pyrolysis of CFRP involves chemical processes that cannot be clearly distinguished from one another, these reactions can take place in overlapping processes [13].

For further analysis, non-destructive testing via computer tomography was used to perform microstructural characterization of the structure following the hot gas test. In addition, the generated images were interpreted using gray scale analysis (Fig 7). Basically, the CT analysis as well as the gray scale analysis is based on the fact that the darker the material present appears in the analysis, the lower its density. Consequently, material components with a high porosity are described with a low gray value. If the low gray values are now correlated with the position of the samples used for the thermogravimetric analysis, it becomes apparent that the areas facing the flow are characterized by low density and high porosity (ρ=0,35g/cm³; Φ=75,19v%). This is also supported by the thermogravimetric analysis (Fig 6), as the front region of the sharp leading edge no longer shows any mass loss and is thus considered to be pyrolyzed. Due to the high carbon content, compared to the material samples from the area at the back in the direction of flow, these samples appear significantly darker than sample 16 (ρ=1,20g/cm³; Φ=10,05v%). A change in the grey scale is particularly evident in the area of the sample with the number 6. This describes the transition from a material area which has not yet been completely pyrolyzed, but which has been exposed to temperatures of over 500°C. The color of the sample in this area is darker than that of sample 16.

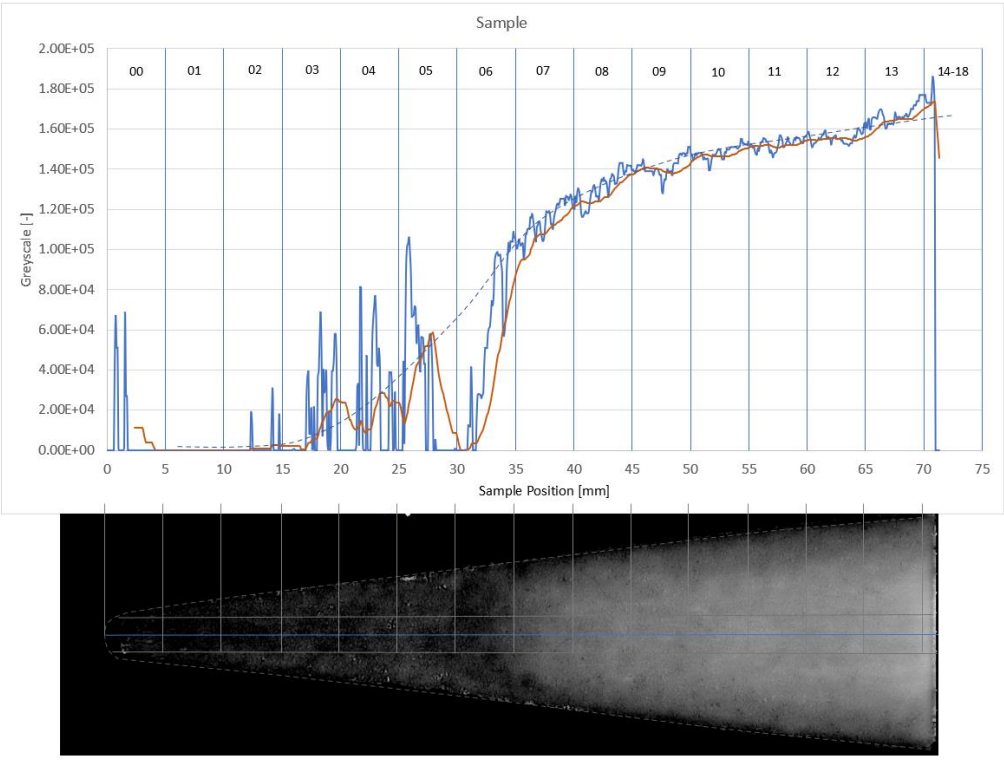

Fig 7. Gray scale analysis of the material tested in the wind tunnel and outlined samples for thermogravimetric analysis

The analysis of the coefficient of thermal expansion can be divided into three different areas (Fig 8) The first area includes a significant increase in CTE, with a decrease in CTE within the second area. In the third area, there is a slight increase in CTE. In the 0° orientation of the fibers (blue), the CTE increases to 8.11x10^-6K^{-1} in the area up to 93°C, after which a decrease in CTE to 0.26x10^-6K^{-1} at 823°C is evident. The analysis of the sample taken from the sample plate at an angle of 90° (red) experiences an increase in CTE up to 113°C, where it is 10.70x10^-6K^{-1}. Following this, the CTE drops to a value of 0.31x10^-6K^{-1} at 1039°C. Noticeable within this curve are two plateaus, the first being in the area between 163°C and 193°C and the second being in the area between 283°C and 343°C. Both of these plateaus include a slight increase in CTE at the end of the plateau.

The steep rise in the curves show thermally induced strains within the material, which are due to the crosslinking reaction of the polymer [13]. The sharp decrease in expansion within the red curve occurs up to the first crosslinking temperature of the polymer, where a small increase in strain can be detected in this region due to the crosslinking reactions. Subsequently, thermal stresses within the material are

relieved [16]. A loss of mass takes place within the material (Fig 8). The second plateau of the curve lies in the region of the second crosslinking peak of the resin system, whereby a renewed expansion can be detected. Since the area of main pyrolysis starts at a temperature of 300°C, the further loss of mass is due to the material pyrolysis taking place. After its completion, the material expansion remains at a constant level.

The vapor pressure of the solvents still in the material is increased, leading to expansion of the sample. When interpreting the measurement, it must be noted that the heating rate of 5K/min was chosen high, which means that the temperature distribution within the sample can be considered inhomogeneous. This can lead to an expansion that is detected as increased [16].

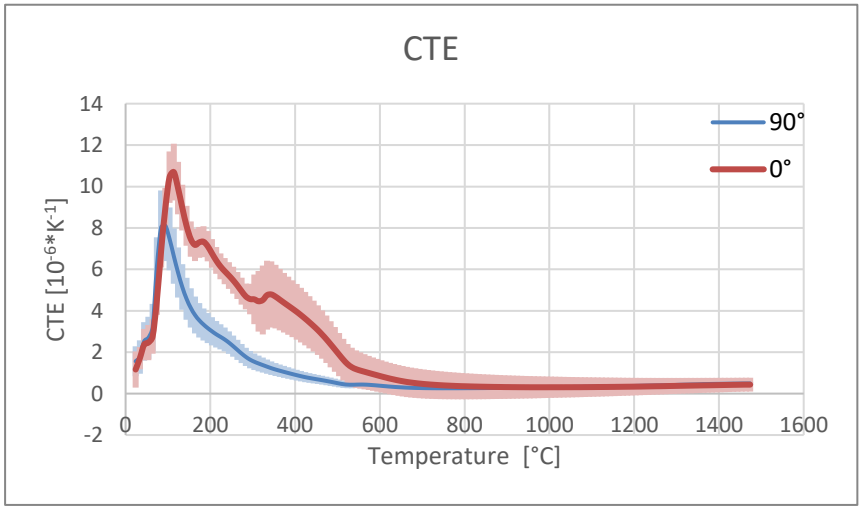

Fig 8. Thermal expansion as a function of the temperature and the fiber angle at 0° and 90°

4.2 Tests in the Wind Tunnel L2K

As mentioned before a specific test condition has been selected to perform experiments in a realistic aerothermal environment. Since standard operation mode of L2K provides high specific enthalpies with significant oxygen dissociation, here nitrogen flow with a small oxygen fraction is used to simulate the target flight conditions at altitudes below 50km correctly. Table 2 contains main flow parameters of tests. At the enthalpy level of 6.85MJ/kg there is no nitrogen dissociation and there the main species of the flow is molecular nitrogen. As shown in the table the small percentage of air added to nitrogen leads to formation of atomic oxygen with a mass fraction of less than 1%. The test duration was 120 seconds.

Table 2. L2K test conditions (Operating Data)

Constraints	Value
Gas Mass Flow Rate	50 [g/s]
Reservoir Pressure	1430 [hPa]
Specific Enthalpy	6.85 [MJ/kg]
Nozzle Throat Diameter	29 [mm]
Nozzle Exit Diameter	100 [mm]
Distance from Nozzle Exit	120 [mm]
Atmosphere: Nitrogen/Air Ratio	24/1
Atomic Oxygen Fraction inside the Flow	approx. 1 [%]
Test Duration	120 [s]

Fig 9 and Fig 10 show video images of the sample in the high enthalpy flow field of L2K. Because of strong emission of the high enthalpy flow behind the leading edge shock, the free stream flow

downstream of the nozzle with high kinetic energy and low temperature is not visible (Fig 9). Three optical windows around the nozzle are used to take video images and to perform pyrometer measurements.

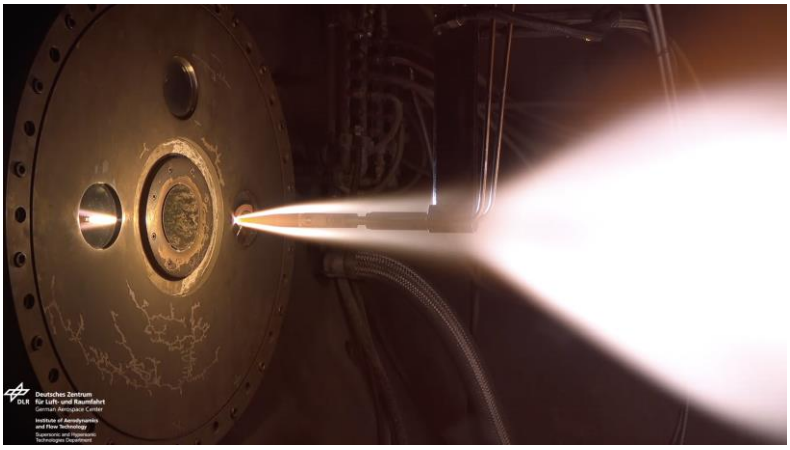

Fig 9. Video image of the test sample in L2K (side view)

The leading edge of the sample became very hot and dominate the emission spectrum even in the visible range (Fig 10). The strong illumination is partially caused by the reflection of the arc heater emission, which hits the sample front surface after passing the nozzle throat.

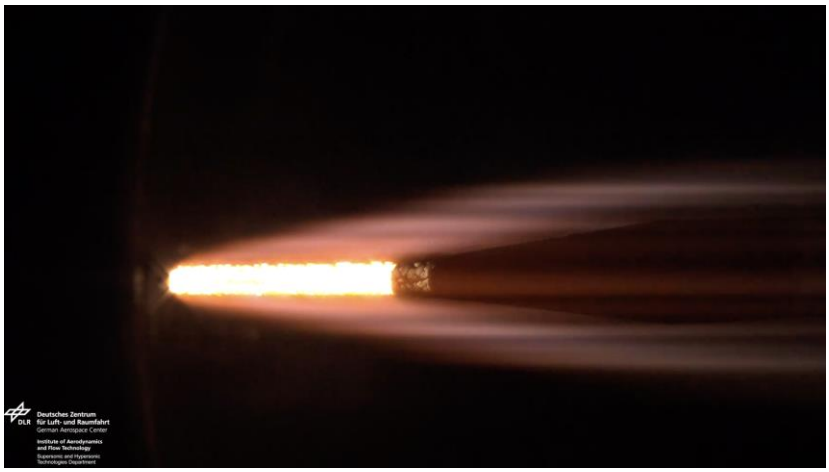

Fig 10. Video image of the test sample in L2K (front view)

The leading-edge surface temperature of the sample was measured using a spectral pyrometer and a two-color pyrometer. The evolution of the temperature over the testing time is included in Fig 11. During the ignition of the arc heater and start of the flow the sample holder is in the background of the test chamber and not exposed to the flow. After completing the setting parameter adjustment and achievement of steady state flow conditions, the test sample is swept into the flow. The time point 0 in Fig 11 indicates the arrival of the sample to the flow axis. At this position the sample surface is also visible to both pyrometers and temperature measurements start. High temperature pyrometers start measuring at temperatures above several hundreds' grad. Depending on the measurement range and spectral range the threshold value varies. The spectral and two-color pyrometers of L2K start measurement at 700°C and 1000°C, respectively.

Roughly 20 seconds after the sample injection into the flow the surface temperature of the leading edge exceeds 2000°C and reaches a level of approx. 2070°C. It stays almost constant over the complete testing time of 120 seconds. After two minutes test at hypersonic conditions the sample is removed from the flow field. It has to be mentioned that the temperature on the side wall remains significantly lower. The expansion of the flow alongside surfaces leads to remarkable decrease of the pressure and heat flux in this region.

At L2K and L3K facilities an optical surface scanner is used to perform contour measurements on test samples before and after each test. This technique is also applied on the sample of edge Rocket Technology. The image in Fig 12 shows clearly that the recession at the leading edge is around 1mm while side surfaces of the material don't show any degradation.

Although a slight leading-edge erosion and typical micro-crack formation resulting from the escape of pyrolysis products of the ablative material through the surface have been noticed, structural integrity of the samples (A and B) contained (Fig 14).

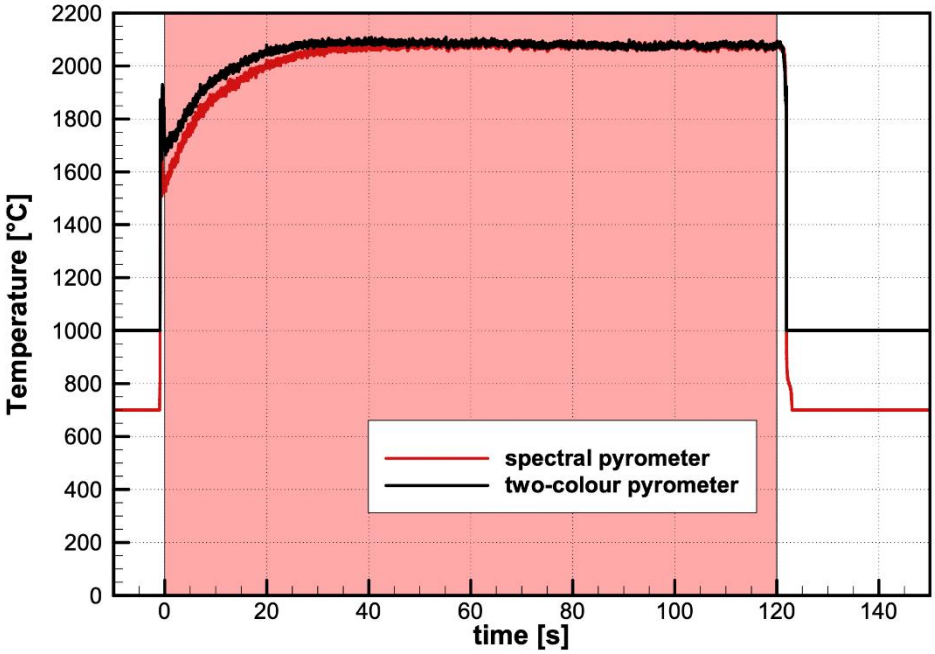

Fig 11. Measured surface temperature during the test

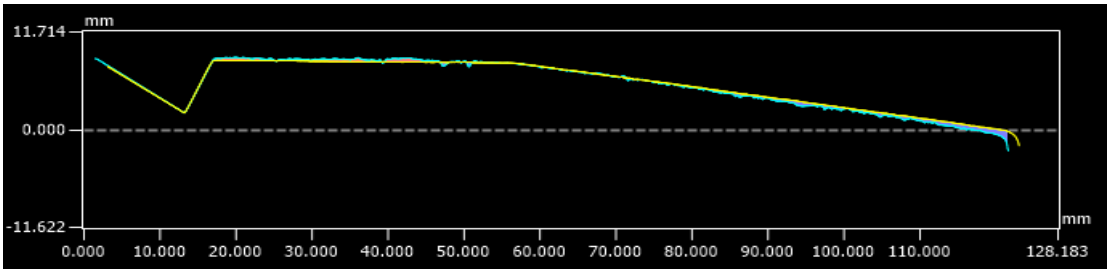

Fig 12. *edgeM13* leading edge before (yellow) and after (turquois) the L2K test in [mm]

5. Conclusion

The complete test assembly, containing the 'edgeM13' leading edge, leading edge interface to the aluminum substructure and the substructures phenolic cork TPS, is successfully qualified in the arc heated facility (L2K). Within the 120sec test duration the 'edgeM13' showed a degradation of around 1mm at the stagnation point without any lateral movement or deformation. The material data is validated and within the required specification, thus it is applicable to manage the thermo-mechanic loads in full scale in combination with standard metallic or CFRP substructures.

To evaluate the full sample test cycle, the first test FEA (Fig 1) is extended back to room temperature without additional heat load. Once the sample is out of the flow, the stored thermal energy is heating through the sample, especially the high temperature area from the stagnation point.

The overall max. temperature at each element is evaluated and the results are shown in Fig 13 in accordance to the CT measurement and are confirmed by the STA analysis (Fig 6+7).

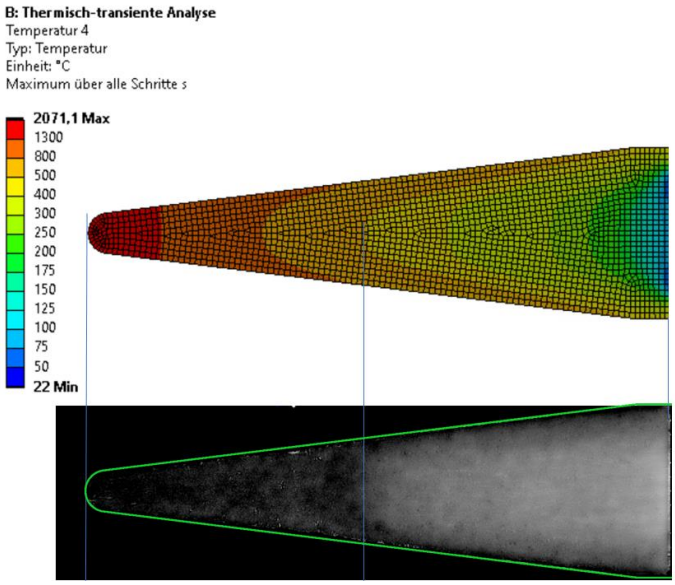

Fig 13. edge Rocket Technology FEA incl. post-test-heating, max. temperature at each element compared to the CT measurement incl. CAD model contour

Both samples (A and B) show the outer optical phases after the test with an approx. 10-15mm edge effects and a 40-50mm constant value in the mid part for a reliable FEA validation.
At the stagnation point pure C/C is visible, followed by the brown phenolic ablation components and the nearly black, high loaded virgin material in the aft end of the leading edge (see chapter 4.1). The leading edge and the bonded cork layer protected the aluminium cold structure and ensured the structural integrity of the assembly.

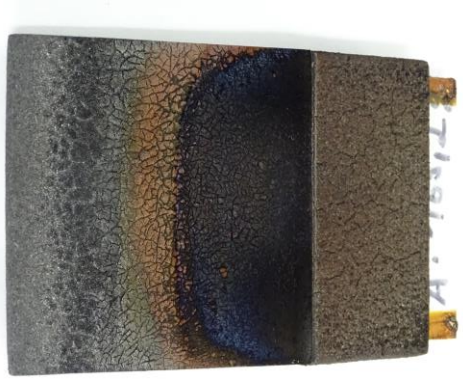

Fig 14. edge Rocket Technology test sample (A) after the L2K test

References

1. Weihs, H.: Sounding Rockets for Entry Research: SHEFEX Flight Test Program. Proceedings of the 21st ESA Symposium on Rocket and Balloon Programmes, SP-721, Pages 143-152. ESA Communications. ISBN 978 92 9092 285 8. (2013).
2. Gülhan, Esser, Koch; Experimental Investigation of Re-entry Vehicle Aerothermodynamic Problems in Arc-Heated Facilities. Journal of Spacecraft and Rockets, Vol. 38, No. 2, p. 199-206, 2001.
3. Esser, Gülhan; Flow Field Characterization of DLR´s Arc Heated Facilities L2K and L3K. Proceedings of the 3rd European Symposium on Aerothermodynamics for Space Vehicles, ESTEC, Netherlands, 1998.
4. Gülhan, Esser; A Study on Heat Flux Measurements in High Enthalpy Flows. 35th AIAA Thermophysics Conference, Paper AIAA 2001-3011, USA, 2001.
5. Koch, U.; Gülhan, A.; Esser, B.; Determination of NO-Rotational and Vibrational Temperature Profiles in a High Enthalpy Flow Field with Nonequilibrium. 1st Joint French-German Symp. of Simulation of Atmospheric Entries by Means of Ground Test Facilities, Stuttgart, 17.-18. November 1999.
6. Del Veccio, A.; Palumbo, G.; Koch, U.; Gülhan, A.; Temperature Measurements by Laser-induced Fluorescence Spectroscopy in Nonequilibrium High Enthalpy Flow. Journal of Thermophysics and Heat Transfer, Vol. 14, No. 2, April-June 2000.
7. Koch, U.; Esser, B.; Gülhan, A.; Two Dimensional Spatially Resolved Two Photon Oxygen Atom Laser Induced Fluorescence Measurements in the Flow Field of the Arc Heated Facility L3K. 5th European Symposium on Aerothermodynamics for Space Vehicles, Cologne, Germany, November 8- 11, 2004.
8. Bertin, J. J.: Hypersonic Aerothermodynamics. American Institute of Aeronautics and Astronautics (AIAA), Inc., Washington, DC (1994)
9. Heppenheimer, T. A.: Facing the Heat Barrier: A History of Hypersonics. National Aeronautics and Space Administration (NASA), Washington, DC (2007)
10. ESA Requirements and Standards Division.: ECSS-E-ST-32-10C Rev.2. https://ecss.nl/standard/ecss-e-st-32-10c-rev-2-structural-factors-of-safety-for-spaceflight-hardware-15-may-2019/. Accessed 15. May 2019
11. Zweben, Carl H., Beaumont P.: Comprehensive Composite Material II. Elsevier Ltd., Amsterdam (2018)
12. Breede, F., Forschungsbericht 2017-61, Deutsches Zentrum für Luft-und Raumfahrt e.V., Köln (2017)
13. Schulte-Fischedick, J., Forschungsbericht 2005-21, Deutsches Zentrum für Luft-und Raumfahrt e.V., Köln (205)
14. Trick, K. A., et.Al., A KINETIC MODEL OF THE PYROLYSIS OF PHENOLIC RESIN IN A CARBON/PHENOLIC COMPOSITE, Carbon Vol. 35, No.3, pp. 393-401, Elsevier Science Ltd., Great Britain (1997)
15. Kimberly, A., et.Al., MECHANISMS OF THE PYROLYSIS OF PHENOLIC RESIN IN A CARBON/PHENOLIC COMPOSITE, Carbon Vol. 33 No. 11, pp. 1509-1515, Elsevier Science Ltd., Great Britain (1995)
16. Mottram, J. T., et.Al., Thermal expansion of phenolic resin and phenolic-fibre composites, Journal of materials science 27, pp 5015-5026, Capman & Hall 1992